*Progress In Electromagnetics Research Letters, Vol. 46, 19–24, 2014*

# Design of a Wideband Planar Microstrip-Fed Quasi-Yagi Antenna

**Hao Wang*, Shu-Fang Liu, Wen-Tao Li, and Xiao-Wei Shi**

**Abstract**—A compact wideband planar microstrip-fed quasi-Yagi antenna is presented. In order to achieve a high gain, the traditional rectangular director in one row is replaced by two rows of directors with an angle, and the overall size of the antenna is unchanged. By adjusting the angle between the two rows of directors, a better performance is achieved. The measurement results show that a broadband impedance about 85.5% (1.84–4.59 GHz) for $S_{11}$ less than $-10$ dB and a gain about 4.5–9.3 dBi are obtained. Simulation and measurement results are provided and discussed. The agreements between the simulation and measurement results indicate that the antenna is suitable for wireless communication applications and phased arrays.

## 1. INTRODUCTION

Printed quasi-Yagi antennas have attracted much attention for using in microwave and millimeter-wave applications because of their low manufacturing cost, low profile, broadband, high gain, ease of integration with monolithic microwave integrated circuits (MMIC), and the ability to be mounted on planar, nonplanar, and rigid exteriors. In general, a printed quasi-Yagi antenna consists of four parts: reflector, driver, directors and feeding structure and the bandwidth of the antenna has been considered to be largely determined by the feeding network. Based on this principle, some broadband antennas with different feeding structures have been proposed. Kaneda et al. described a quasi-Yagi antenna fed by a microstripline-to-coplanar stripline (MS-to-CPS) transition balun [1–3]. However, this balun produced only a stable radiation pattern of the antenna near the center frequency of operation. J. Sor et al. presented a coplanar waveguide-to-coplanar-strip (CPW-to-CPS) transition balun in [4, 5] and a broad bandwidth of 30% at X-band was obtained in [4]. A microstrip-to-slotline transition (MS-to-ST) was proposed in [6], and a measured bandwidth approximately 46% was achieved. Other feeding structures such as artificial transmission line based MS-to-CPS transition balun or tapered line, MS-fed, CPW-fed were proposed in [7–11]. However, those complex feeding structures would not only increase design complexity but also increase the size of the antenna.

In [12], a simple feeding structure was proposed, and broadband impedance bandwidth of 43.2% was obtained. Here, based on the presented antenna in [12], a modified Yagi-antenna with wideband is proposed. Moreover, in order to overcome the property of low gain, each director in [12] is divided into two, and they are distributed at both sides of the dielectric symmetrically. Through optimizing the size of the new directors and the angle between the two rows of directors, an improvement gain about 4.5–9.3 dBi over the whole operating bandwidth is achieved. Furthermore, the impedance bandwidth of the antenna is approximately 85.5% (1.84–4.59 GHz). Prototypes are fabricated to validate the design. The agreements between the simulation and measurement results indicate that the proposed antenna may be very useful for wireless communication applications and phased arrays.

*Received 17 March 2014, Accepted 11 April 2014, Scheduled 1 May 2014*
* Corresponding author: Hao Wang (wang_haohaha@126.com).
The authors are with the Science and Technology on Antenna and Microwave Laboratory, Xidian University, Xi'an 710071, China.

## 2. ANTENNA DESIGN AND PARAMETERS ANALYSIS

### 2.1. Antenna Design

Figure 1 shows the structure and photograph of the proposed quasi-Yagi antenna. The proposed antenna has a structure printed on a single-layer FR4 dielectric substrate, which has permittivity of 4.4 with thickness of 1.6 mm, and a total substrate size of $L \times W = 94 \times 50\,\text{mm}^2$. The antenna consists of four mainly parts: reflectors, driver, directors and feeding structure. In order to obtain a wideband, the traditional reflector of rectangular shape is replaced by two reflectors of C-shape, which are at the top and bottom layer of the substrate, respectively. The rectangular driver (D) is excited by a simple microstrip line. The width of the microstrip line is calculated to achieve the $50\,\Omega$ characteristic impedance feeding line. In order to further excavate the potential of the antenna without increasing the size of the antenna, the traditional rectangular directors are divided into two. The 12 directors with different sizes are distributed at both sides of the $y$-axis symmetrically. The angle between of the two rows of directors is given by $\theta$, as shown in Fig. 1(a). By optimizing the geometrical size of the proposed antenna with Ansoft HFSSv13.0, a broad operating bandwidth antenna is obtained, and Table 1 gives the optimized dimensions of the proposed antenna.

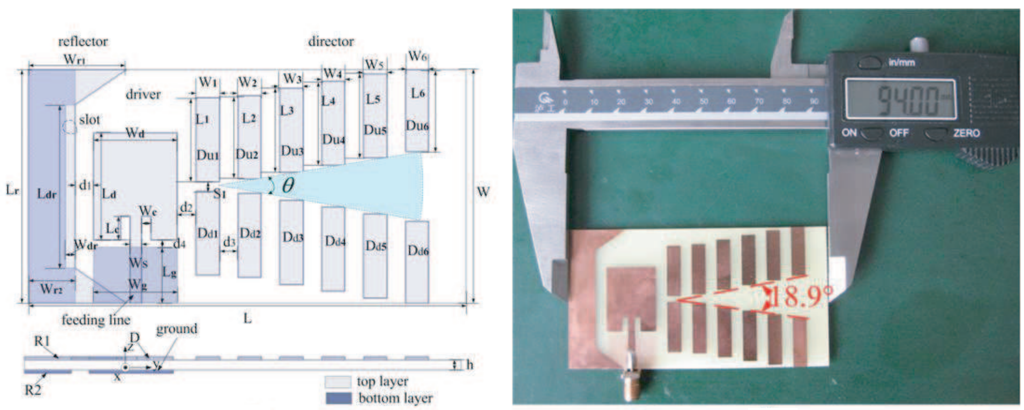


(a) (b)

**Figure 1.** (a) Structure of the proposed antenna. (b) Photograph of the proposed antenna.

**Table 1.** Geometrical size of the proposed antenna (units: mm).

| $L$ | $W$ | $Lr$ | $Wd$ | $Ld$ | $Wr1$ | $Wr2$ | $Ldr$ |
|---|---|---|---|---|---|---|---|
| 94 | 50 | 50 | 18 | 23 | 21 | 10 | 21 |
| $Wdr$ | $Lg$ | $Wg$ | $Ls$ | $Ws$ | $W1$ | $L1$ | $W2$ |
| 2 | 18 | 12 | 5 | 2 | 5 | 16 | 5 |
| $L2$ | $W3$ | $L3$ | $W4$ | $L4$ | $W5$ | $L5$ | $W6$ |
| 16 | 5 | 16 | 5 | 16 | 5 | 16 | 5 |
| $L6$ | $d1$ | $d2$ | $d3$ | $d4$ | $s1$ | $h$ | $\theta$ |
| 13.75 | 4 | 5 | 5 | 3 | 3 | 1.6 | 18.9 |

### 2.2. Effects of C-Shape Reflector on Antenna Performance

From Fig. 1, it can be seen that the whole structure is similar to the one mentioned in [12] except the reflectors. However, it is no other than those differences that improve the bandwidth significantly. In order to analyze the influence of the C-shaped reflector on the impedance bandwidth, Fig. 2 shows the reflection coefficient of the antenna for various $Wr1$. All variables are initially set to the optimized

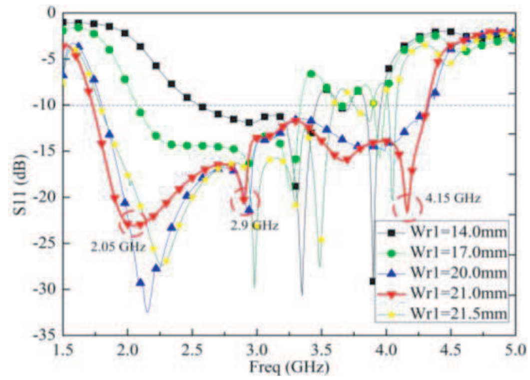


**Figure 2.** Reflection coefficient of the antenna for various $Wr1$.

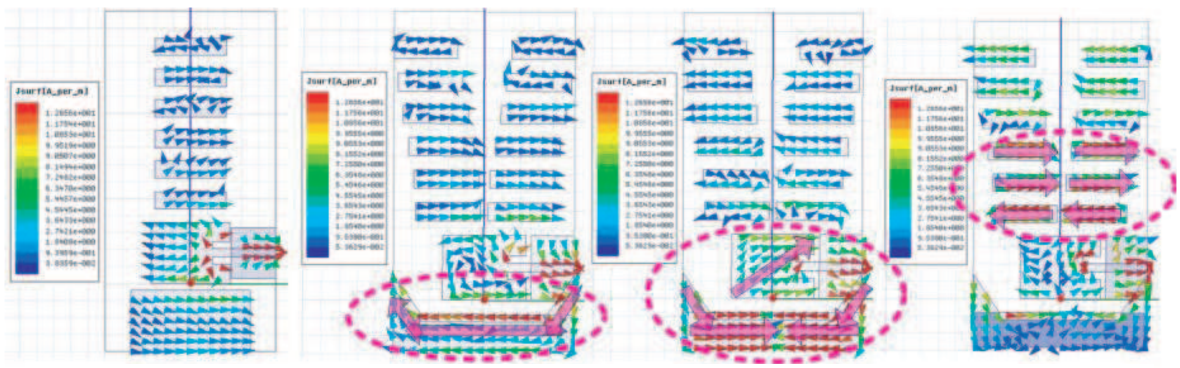

(a) (b) (c) (d)

**Figure 3.** Simulated surface current distribution. (a) Reference [12] 2.05 GHz. (b) Proposed antenna 2.05 GHz. (c) Proposed antenna 2.90 GHz. (b) Proposed antenna 4.15 GHz.

values discussed in last section. From this figure, it is seen that an increase in $Wr1$ improves the performance of the antenna at low frequency. When $Wr1$ is equal to 21 mm, both a C-shaped reflector and the widest bandwidth are achieved.

Compared with the $S_{11}$ curve of the antenna in [12], it is seen from Fig. 2 that a new resonant frequency point, namely, 2.05 GHz, is produced by the C-shaped reflector. Fig. 3 presents the simulated surface current distributions of the proposed antenna at three resonant frequency points shown in Fig. 2. The surface current distribution at 2.05 GHz of the antenna in [12] is also given in Fig. 3 to show the performance of the C-shape reflector. From Fig. 3(a), it is seen that the current mainly focuses on the feeding line, which means that little energy is radiated into free space. As shown in Fig. 3(b), the current mainly focuses on the C-shape reflector and presents a long current path, which can explain the reason that the C-shaped reflector can broaden the operating band at low frequency. Fig. 3(c) shows the surface current distribution of the antenna at 2.9 GHz. It is seen that the current mainly focuses on the C-shaped reflector and the rectangular driver. But compared with the current path of the antenna at 2.05 GHz, a shorter current path is presented. Meanwhile, the intensity of the current at 2.9 GHz is larger than that of the antenna at 2.05 GHz. So it is easy to predict that a higher gain at 2.9 GHz can be obtained. In Fig. 3(d), the current mainly focuses on the first six directors and presents the shortest current path, which is in good agreement with the operating frequency.

### 2.3. Effects of the Angle $\theta$ and Two Rows of Directors on the Antenna Performance

In order to further excavate the potential of the proposed antenna without increasing the size of the antenna, each director is divided into two. The relative position and size of the 12 directors are controlled

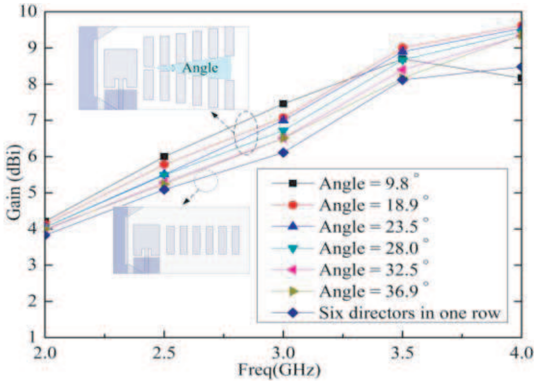


**Figure 4.** Simulated gain of the antenna for various angle $\theta$

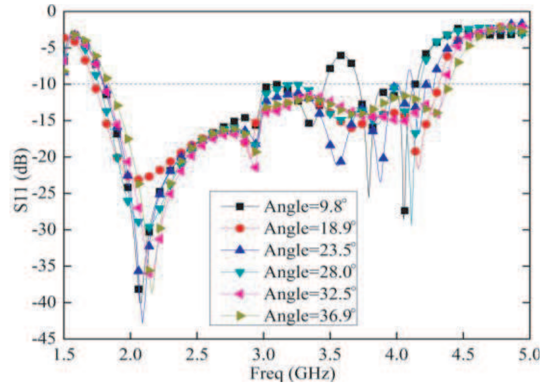


**Figure 5.** Reflection coefficient of the antenna for various angle $\theta$.

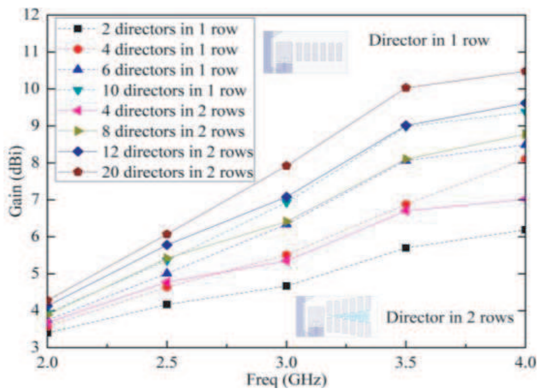


**Figure 6.** Simulated gain of the antenna for different number of directors.

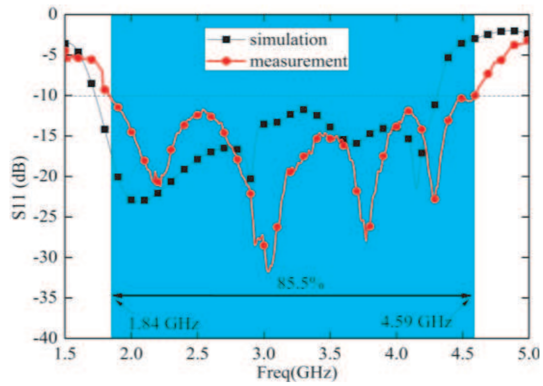


**Figure 7.** Simulated and measured reflection coefficient curves of the proposed antenna.

by the flare angle $\theta$. Fig. 4 and Fig. 5 give the gain and reflection coefficient curves of the antenna for different values of $\theta$. In order to analyze the performance of two rows of directors, the gain of the antenna with six directors in one row is also shown in Fig. 4. From Fig. 4, it is seen that the gain of the antenna with 6 directors is smaller than that of the antenna with 12 directors, because the antenna with 12 directors has larger effective aperture. Meanwhile, the value of angle $\theta$ has great effect on the antenna gain but little influence on the reflection coefficient. When $\theta$ equals 9.8°, the antenna has the highest gain at low frequency but the lowest gain at high frequency. The reason for this phenomenon is that a smaller angle leads to a larger size of all the directors, which results in a larger leading role at low frequency, but the larger director acts as reflectors at high frequency. As shown in Fig. 4 and Fig. 5, when $\theta$ is equal to 18.9°, both high gain and broad bandwidth are obtained.

In order to further illustrate the performance of two rows of directors, some simulation based on the antenna with different numbers of directors is performed, as shown in Fig. 6. The antenna with 4/8/12/20 directors in two rows has the same size as the antenna with 2/4/6/10 directors in one row, respectively. Referring to Fig. 6, for antenna with the same size, the antenna with two rows of directors shows a higher gain, which means that the design has certain adaptability and can be used in other antenna designs.

## 3. EXPERIMENTAL RESULTS

To validate the design, prototypes of the proposed antenna are fabricated and measured. For the return loss measurement, an edge-mount SMA connector was soldered to the edge of the board, as shown in Fig. 1(b). The reflection coefficient was measured on the Agilent Technologies N5230A vector network analyzer. The simulated and measured reflection coefficient curves against frequency of the proposed antenna are shown in Fig. 7. It can be observed from the figure that the measured impedance bandwidth is about 85.5%, ranging from 1.84 GHz to 4.59 GHz. The shift in frequency between the simulated and measured results can possibly be attributed to a small tolerance in the substrate and/or overetching of the metal.

Figure 8 illustrates the normalized measured and simulated radiation patterns at 2.0, 3.0 and 4.0 GHz. Referring to Fig. 8, except back lobes of the patterns, the agreement between the simulated and measured results is fairly good, and the front-to-back rations are basically above 10 dB at the desired frequencies. The measured and simulated gains and the radiation efficiency of the proposed antenna are presented in Fig. 9. The measured gain is about 4.5–9.3 dBi over the operating band. It

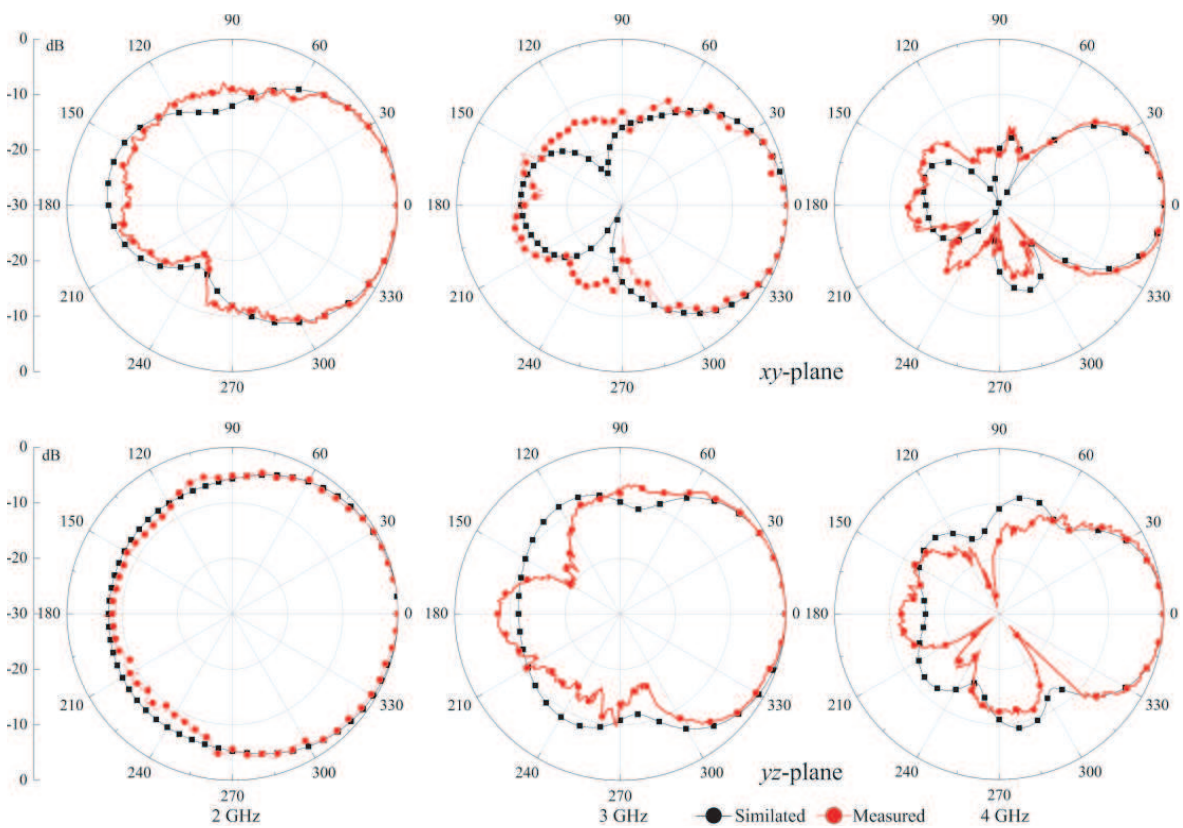


**Figure 8.** Simulated and measured normalized radiation patterns of the antenna.

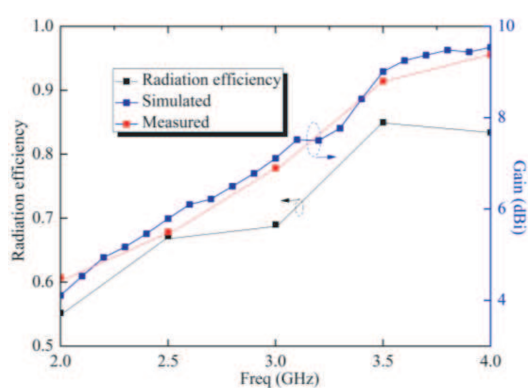


**Figure 9.** Simulated and measured gain and radiation efficiency of the antenna.

can be seen that a good agreement between simulated and measured results is obtained. Here the large variation in gain can be vanished by decreasing the number of the director, namely, the length ($L$) of the antenna. Meanwhile, as shown in this figure, an average radiation efficiency about 75% is achieved.

## 4. CONCLUSION

In this paper, a broadband planar microstrip-fed quasi-Yagi antenna is proposed and studied. First, by changing the shape of the reflector, a wideband performance is obtained. Second, in order to further excavate the potential of the antenna, the traditional director in one row is replaced by two rows of directors, with the antenna size unchanged. The overall size of the antenna is $94 \times 50\,\mathrm{mm}^2$. The measured results show that the antenna has a wide impedance bandwidth about 85.5%, ranging from 1.84 GHz to 4.59 GHz. The gain of the antenna is about 4.5–9.3 dBi, and an average radiation efficiency about 75% is achieved. The agreements between the simulation and measurement results indicate that the proposed antenna is suitable for wireless communication applications, such as WLAN, WCDMA, LTE.

## ACKNOWLEDGMENT

This work was supported by the National Natural Science Foundation of China under Grant 61101069.

## REFERENCES

1. Kaneda, N., W. Deal, Y. Qian, R. Waterhouse, and T. Itoh, "A broadband planar quasi-Yagi antenna," *IEEE Transactions on Antennas and Propagations*, Vol. 50, No. 8, 1158–1160, Aug. 2002.
2. Avila-Navarro, E., A. Segarra-Martinez, J. A. Carrasco, and C. Reig, "A low-cost compact uniplanar quasi-Yagi printed antenna," *Microwave and Optical Technology Letters*, Vol. 50, No. 3, 731–735, Mar. 2008.
3. Ta, S. X., H. Choo, and I. Park, "Wideband double-dipole Yagi-UDA antenna fed by a microstrip-slot coplanar stripline transition," *Progress In Electromagnetics Research B*, Vol. 44, 71–87, 2012.
4. Sor, J., Y. Qian, and T. Itoh, "Coplanar waveguide fed quasi-Yagi antenna," *Electronics Letters*, Vol. 36, No. 1, 1–2, Jan. 2000.
5. Ding, Y., Y.-C. Jiao, B. Li, and L. Zhang, "Folded triple-frequency quasi-Yagi-type antenna with modified CPW-to-CPS transition," *Progress In Electromagnetics Research Letters*, Vol. 37, 143–152, 2013.
6. Ta, S. X., B. Kim, H. Choo, and L. Park, "Wideband quasi-Yagi antenna fed by microstrip-to-slotline transition," *Microwave and Optical Technology Letters*, Vol. 54, No. 1, 150–153, Jan. 2012.
7. Kan, H., R. Waterhouse, A. Abbosh, et al., "Simple broadband planar CPW-fed quasi-Yagi antenna," *IEEE Antennas and Wireless Propagtation Letters*, Vol. 6, 18–20, 2007.
8. Han, K., Y. Park, H. Choo, and I. Park, "Broadband CPS-fed Yagi-Uda antenna," *Electronics Letters*, Vol. 45, No. 24, 1207–1209, Nov. 2009.
9. Wang, Z., X. L. Liu, Y.-Z. Yin, J. H. Wang, and Z. Li, "A novel design of folded dipole for broadband printed Yagi-Uda antenna," *Progress In Electromagnetics Research C*, Vol. 46, 23–30, 2014.
10. Ma, T. G., C. W. Wang, R. C. Hua, and J. W. Tsai, "A modified quasi-Yagi antenna with a new compact microstrip-to-coplanar strip transition using artificial transmission lines," *IEEE Transactions on Antennas and Propagations*, Vol. 57, No. 8, 2469–2474, Aug. 2009.
11. Mohammed, J. R., "Design of printed Yagi antenna with additional driven element for WLAN application," *Progress In Electromagnetics Research C*, Vol. 37, 67–81, Jan. 2013.
12. Lu, H. D., L. M. Si, and Y. Liu, "Compact planar microstrip-fed quasi-Yagi antenna," *Electronics Letters*, Vol. 48, No. 3, 140–141, Feb. 2012.